EPiC Series in Computing

Volume 108, 2025, Pages 15–38

Proceedings of 12th Int. Workshop on Applied Verification for Continuous and Hybrid Systems


# ARCH-COMP25 Category Report: Continuous and Hybrid Systems with Linear Continuous Dynamics

Matthias Althoff[1], Marcelo Forets[2], Maximilian Perschl[1], and Christian Schilling[3]

[1] Technical University of Munich, Department of Computer Engineering, Munich, Germany
althoff@in.tum.de, max.perschl@tum.de
[2] Universidad de la República, Montevideo, Uruguay
mforets@gmail.com
[3] Aalborg University, Aalborg, Denmark
christianms@cs.aau.dk

**Abstract**

We present the results of the ARCH[1] 2025 friendly competition for formal verification of continuous and hybrid systems with linear continuous dynamics. In its ninth edition, two tools participated to solve eight different benchmark problems in the category for linear continuous dynamics (in alphabetical order): CORA and JuliaReach. This report is a snapshot of the current landscape of tools and the types of benchmarks they are particularly suited for. Due to the diversity of problems, we are not ranking tools.

## 1 Introduction

**Disclaimer** The presented report of the ARCH friendly competition for *continuous and hybrid systems with linear continuous dynamics* aims at providing a landscape of the current capabilities of verification tools. We would like to stress that each tool has unique strengths—not all of the specificities can be highlighted within a single report. To reach a consensus in what benchmarks are used, some compromises had to be made so that some tools may benefit more from the presented choice than others.

We consider the verification of hybrid systems (i.e., mixed discrete/continuous systems) with linear continuous dynamics

$$\dot{x}(t) = Ax(t) + Bu(t),$$

[1] Workshop on Applied Verification for Continuous and Hybrid Systems (ARCH), cps-vo.org/group/ARCH

where $A \in \mathbb{R}^{n \times n}$, $x \in \mathbb{R}^n$, $B \in \mathbb{R}^{n \times m}$, and $u \in \mathbb{R}^m$. For all results reported by each participant, we have run an independent repeatability evaluation. To establish further trustworthiness of the results, the code with which the results have been obtained is publicly available at gitlab.com/goranf/ARCH-COMP. The selection of the benchmarks has been conducted within the forum of the ARCH website (cps-vo.org/group/ARCH), which is visible for registered users and registration is open to anybody. All tools presented in this report use some form of reachability analysis. This, however, is not a constraint set by the organizers of the friendly competition. We hope to encourage further tool developers to showcase their results in future editions. All tools are run on the same machine.

## 2 Participating Tools

The tools participating in the category *Continuous and Hybrid Systems with Linear Continuous Dynamics* are subsequently introduced in alphabetical order.

**CORA** (Matthias Althoff, Mark Wetzlinger) The tool *COntinuous Reachability Analyzer* (CORA) [2, 5, 6, 4, 25, 11, 37] realizes techniques for reachability analysis with a special focus on developing scalable solutions for verifying hybrid systems with nonlinear continuous dynamics and/or nonlinear differential-algebraic equations. A further focus is on considering uncertain parameters and system inputs. Due to the modular design of CORA, much functionality can be used for other purposes that require resource-efficient representations of multi-dimensional sets and operations on them. CORA is implemented as object-oriented MATLAB code and is available at cora.in.tum.de.

**JuliaReach** (Marcelo Forets, Christian Schilling) JuliaReach [17] is an open-source software suite for reachability computations of dynamical systems, written in the Julia language and available at `http://github.com/JuliaReach`. The core library is ReachabilityAnalysis.jl. For the set computations, we use our LazySets.jl library [23]. JuliaReach can analyze systems in either continuous-time or discrete-time semantics. For some of the models, we use our custom parser for SpaceEx model files, and otherwise we create the models in Julia. In this competition, we use the following algorithms: `BFFPSV18` (based on the support function on low-dimensional subspaces [18, 16]), `GLGM06` (based on zonotopes [27]), `ASB07` (based on zonotopes for parametric systems [10]), and `LGG09` (based on the support function [29]). These algorithms can be combined with different *approximation models* [24], such as forward and correction hull, adapted from [16] and [1], respectively. For hybrid systems with time-triggered transitions, we use the algorithm from [22].

## 3 Verification of Benchmarks

For the 2025 edition, we decided to add more challenging random examples compared to our 2024 friendly competition [12].

**Special Features** We briefly list the special features of each benchmark:

- *Heat 3D* benchmark from [14]: This is a purely continuous benchmark resulting from a spatial discretization of a heat partial differential equation in three dimensions. The system can be scaled from a $5 \times 5 \times 5$ mesh (125 dimensions) to a $100 \times 100 \times 100$ mesh (one million dimensions), each variation being roughly an order of magnitude apart.

- *Clamped beam* benchmark from [30, Sec. 4.2]: This purely continuous benchmark models a spatially discretized beam clamped on one end and pulled on the other end yielding interesting oscillations. The system dimension ranges from 200 to 2000 depending on the number of nodes used for the discretization. A challenge of this benchmark is that it has very little damping.

- *Spacecraft rendezvous* benchmark from [19]: This benchmark has hybrid dynamics and is a linearization of a benchmark in the other ARCH-COMP category *Continuous and Hybrid Systems with Nonlinear Dynamics*. Consequently, the reader can observe the difference in computation time and verification results between the linearized version and the original dynamics.

- *Random* benchmark from [35]: Purely continuous benchmarks are automatically generated. These benchmarks are unknown to the tool developers so that the tools have to solve them fully automatically. This year, the random problems had up to 1000 continuous state variables.

- *Powertrain* benchmark from [7, Sec. 6]: This is a hybrid system for which one can select the number of continuous state variables and the size of the initial set. Up to 51 continuous state variables are considered.

- *Platooning* benchmark from [15]: A rather small number of continuous state variables is considered, but one can arbitrarily switch between two discrete states: a normal operation mode and a communication-failure mode.

- *Gearbox* benchmark from [20]: This benchmark has the smallest number of continuous state variables, but the reachable set does not converge to a steady state and the reachable set for one point in time might intersect multiple guards at once.

- *Brake* benchmark from [34]: This hybrid benchmark has a time-triggered discrete transition that has to be taken 1,001 times.

**Types of Inputs** Generally, we distinguish between three types of inputs:

1. Fixed inputs, where $u(t)$ is precisely known. In some cases, $u(t) = \texttt{const}$ as in the gearbox benchmark.

2. Uncertain but constant inputs, where $u(t) \in \mathcal{U} \subset \mathbb{R}^m$ is uncertain within a set $\mathcal{U}$, but each uncertain input is constant over time: $u(t) = \texttt{const}$.

3. Uncertain, time-varying inputs $u(t) \in \mathcal{U} \subset \mathbb{R}^m$ where $u(t) \neq \texttt{const}$. Those systems do not converge to a steady state solution and consider uncertain inputs of all frequencies. For tools that cannot consider arbitrarily varying inputs, we mention that changes in inputs are only considered at fixed points in time.

**Different Paths to Success** When tools use a fundamentally different way of solving a benchmark problem, we add further explanations.

**Computation Time** The computation times specified in this report include the computation time of the reachable set and the time needed for the verification of the specifications.

## 3.1 Heat3D

### 3.1.1 Model

Using a mesh, the Heat3D benchmark is a spatially-discretized partial differential equation (PDE) for heat transfer in three dimensions, resulting in ordinary differential equations (ODEs), where each variable represents a mesh point. Depending on the granularity of the discretization, one can adjust the number of variables. This system has no switching or inputs and serves to evaluate the scalability with respect to the number of system dimensions. It is an academic example, although modifications, such as external inputs or more complicated specifications, can be added in the future. This benchmark was used in [14] and is based on a 2D version originally described and evaluated in [28].

All of the sides of the considered heated block are insulated, except the $x = 1$ edge, causing heat exchange with the ambient environment with a heat exchange constant of 0.5. A heated initial region is present in the region, where $x \in [0.0, 0.4]$, $y \in [0.0, 0.2]$, and $z \in [0.0, 0.1]$. The entire initial heated region is the same temperature, which is nondeterministic and chosen in the range 0.9 to 1.1, with the remaining material initially at temperature 0.0. The system dynamics is given by the heat equation PDE $u_t = \alpha^2(u_{xx} + u_{yy} + u_{zz})$, where $\alpha = 0.01$ is the diffusivity of the material.

A linear model of the system is obtained using the semi-finite difference method, discretizing the block with an $m \times m \times m$ grid. This results in an $m^3$-dimensional linear system describing the evolution of the temperature at each mesh point.

Due to the initially heated region, we expect the temperature at the center of the block to first increase, and then decrease due to the heat loss along the $x = 1$ edge. Further, the discretization error increases for smaller $m$, motivating the higher-dimensional versions of the benchmark. The time bound is $T = 40$. For discrete-time tools, the step size 0.02 is used.

### 3.1.2 Specifications

The goal is to find the maximum temperature reached at the center of a $1 \times 1 \times 1$ block, where one edge of the block is initially heated. This can be converted to a safety verification problem by checking that $T_{\max}$ is reachable but $T_{\max} + \delta$ is not, for some small $\delta$ like $10^{-4}$.

There are five suggested sizes, roughly each one an order of magnitude apart in terms of the number of dimensions. The higher-dimensional versions usually prevent explicitly representing the dynamics as a dense matrix in memory. Storing a million by million dense matrix requires a trillion numbers, which at 8 bytes per double-precision number would require eight terabytes of storage.

HEAT01 $5 \times 5 \times 5$ (125 dimensions). Note: the initial set is modified to be heated when $z \in [0.0, 0.2]$ (single mesh point), since that is the best we can do with this granularity. $T_{\max}$: 0.10369 at time 9.44.

HEAT02 $10 \times 10 \times 10$ (1000 dimensions). $T_{\max}$: 0.02966 at time 25.5.

HEAT03 $20 \times 20 \times 20$ (8000 dimensions). $T_{\max}$: 0.01716 at time 22.62.

HEAT04 $50 \times 50 \times 50$ (125,000 dimensions). $T_{\max}$: 0.01161 at time 18.88.

HEAT05 $100 \times 100 \times 100$ (1,000,000 dimensions). $T_{\max}$: 0.01005 at time 17.5.

### 3.1.3 Results

Plots for the $5 \times 5 \times 5$ case are shown in Figure 1. Results are shown in Table 1.

**Note CORA** CORA applies the fully automated verification algorithm in [36] for the benchmark instances HEAT01 and HEAT02. For the higher-dimensional benchmark instances HEAT03 and HEAT04 we compute the reachable set using the Krylov-subspace-based reachability algorithm in [3] using a zonotope order of 2 and an adaptive time-step size based on an updated algorithm which is to be published soon.

**Note JuliaReach** We use the `LGG09` algorithm. We use step sizes 0.025 (HEAT01) resp. 0.015 (HEAT02). For HEAT03 and HEAT04, we lazily compute the matrix exponential using the Lanczos algorithm [32] with Krylov subspace dimension 81 and 131, respectively.

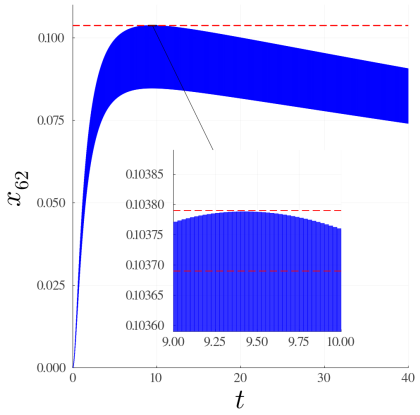


Figure 1: Heat3D: Reachable sets obtained by JuliaReach for the temperature at the center of the block over time for benchmark version HEAT01.

Table 1: Computation Times for the Heat3D Benchmark in [s].

| **tool** | **HEAT01** | **HEAT02** | **HEAT03** | **HEAT04** | **HEAT05** | **language** |
|---|---|---|---|---|---|---|
| CORA | 0.24 | 3.77 | 49.2 | 2447 | – | MATLAB |
| JuliaReach | 0.07 | 2.87 | – | – | – | Julia |
| | *discrete-time tools* | | | | | |
| JuliaReach | 0.02 | 0.7 | 97 | 3217 | – | Julia |

## 3.2 Clamped Beam

### 3.2.1 Model

Similarly to the Heat3D benchmark, the Clamped Beam benchmark [30, Sec. 4.2] also results from the spatial discretization of a partial differential equation (PDE), where each variable represents a node along the beam. The number of states scales proportionally with the number of nodes used for the discretization and the system is influenced by a single external input.

A beam of length $L$ is fixed at one end, while an external load $F(t)$ acts on the other end. Further model parameters are the cross-section area $A$ as well as the Young modulus $E$ and the density $\rho$ of the material. The governing PDE models the displacement $u(x,t)$ as a function of the position $x$ along the beam and the time $t$: $EAu_{xx} - \rho A u_{tt} = 0$. Here the indices indicate partial derivatives with respect to the indexed variables. To obtain a linear system, the beam is spatially discretized using $N$ nodes from $x = 0$ to $x = L$ depending on the stiffness matrix $K \in \mathbb{R}^{N\times N}$ and the mass matrix $M \in \mathbb{R}^{N\times N}$. The original model is extended by introducing a damping matrix $D = aK + bM$, where $a = b = 10^{-6}$, to model a more realistic beam. Rewriting the equation into a first-order system of linear ODEs yields a system dimension of $2N$ describing the displacement and velocity of each node over time. The sparsity pattern reveals four blocks of size $N \times N$: The block (1,1) is all-zero, the block (1,2) is the identity matrix, and the blocks (2,1) and (2,2) are tridiagonal matrices.

The initial condition is chosen such that all nodes have displacement and velocity zero, i.e., $\forall x \in [0, L] : u(x, 0) = 0, u_t(x, 0) = 0$. The boundary condition keeps the displacement at the fixed end zero at all times so that $\forall t : u(0, t) = 0$. The load is modeled by $F(t) = 10000\, H(t)$ with $H(t)$ denoting the Heaviside function. Finally, the time horizon is set to $T = 0.01$. For discrete-time tools, the step size $9.88 \cdot 10^{-7}$ is used.

### 3.2.2 Specifications

The maximum velocity reached at the position $x = 0.7L = 1.7N$ should be below 76.

CB01 $N = 100$ (200 dimensions).

CB02 $N = 500$ (1000 dimensions).

CB03 $N = 1000$ (2000 dimensions).

The load $F(t)$ is modeled in two different ways:

CBC (constant inputs) The inputs are uncertain only in their initial value and constant over time: $F(0) \in \mathcal{F}$, $\dot{F}(t) = 0$, with $\mathcal{F} = [9900, 10100]$.

CBF (time-varying inputs) The inputs can change arbitrarily over time: $\forall t : F(t) \in \mathcal{F}$, with $\mathcal{F} = [9900, 10100]$.

Note that the load $F(t)$ of the original model is different from the input $u(t)$ to the spatially discretized system $\dot{x}(t) = Ax(t) + u(t)$.

### 3.2.3 Results

Plots for the velocity of the node at $x = 0.7L$ (corresponding to node 70) are shown in Figure 2 over the time interval $t \in [0, 0.01]$. The computation times are shown in Table 2.

**Note CORA** For all instances, CORA uses the fully automated verification algorithm from [36].

**Note JuliaReach** We use the `LGG09` algorithm with the following step sizes: $7{\cdot}10^{-6}$ (CBC01), $10^{-7}$ (CBF01), and $2 \cdot 10^{-6}$ (CBC02). For CBC, we also use Krylov methods to efficiently compute the large matrix exponentials.

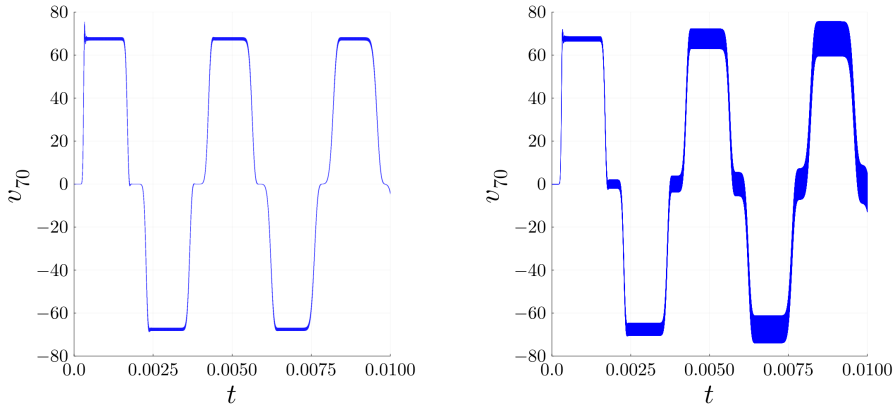


(a) CBC01. (b) CBF01.

Figure 2: Clamped Beam: Reachable sets for the velocity at node 70. All plots are obtained from JuliaReach.

Table 2: Computation Times in [s] for the clamped beam benchmark.

| **tool** | **CBC01** | **CBF01** | **CBC02** | **CBF02** | **CBC03** | **CBF03** | **language** |
|---|---|---|---|---|---|---|---|
| CORA | 0.25 | 0.61 | 4.41 | 7.50 | 49.9 | 93.7 | MATLAB |
| JuliaReach | 0.06 | 2.92 | 1.13 | – | – | – | Julia |
| | *discrete-time tools* | | | | | | |
| JuliaReach | 0.08 | 0.09 | 0.78 | 1.17 | 2.53 | 5.86 | Julia |

## 3.3 Random Benchmarks

### 3.3.1 Model

To evaluate the capabilities of tools without manual tuning by experts, one requires randomly generated benchmarks. To solve the other ARCH benchmarks, tool developers often tune their tools to best solve a given verification task. However, most users of the participating tools typically do not have the knowledge or time to tune algorithms for reachability analysis. Thus, this benchmark category currently best evaluates the performance when a tool is used in practice.

We use the method in [35] for the random generation of benchmarks. These benchmarks are directly created on the server for evaluation and, consequently, are not known to the tool developers in advance. The method in [35] creates challenging benchmarks by placing unsafe sets close to the reachable set. This is done by first computing the reachable set for a provided degree of over-approximation. By placing unsafe sets directly at the border of the reachable set, the approach varies the difficulty by adapting the degree of over-approximation. The same technique is used to create unsatisfiable benchmarks for checking whether unsatisfiability is properly detected. For these benchmarks, under-approximative reachable sets are computed to which the unsafe sets are attached; the difficulty is analogously adapted by changing the amount of under-approximation.

Models are created randomly of the form

$$\begin{aligned}\dot{x}(t) &= Ax(t) + Bu(t)\\ y(t) &= Cx(t) + v(t),\end{aligned}$$

where $x \in \mathbb{R}^n$ is the state vector, $A \in \mathbb{R}^{n\times n}$ is the state matrix, $u \in \mathbb{R}^m$ is the input vector, $B \in \mathbb{R}^{n\times m}$ is the input matrix, $y \in \mathbb{R}^r$ is the output vector, $C \in \mathbb{R}^{r\times n}$ is the output matrix, and $v \in \mathbb{R}^r$ is the sensor noise. The linear system is generated randomly according to [35, Alg. 1]. This algorithm creates the system matrices $A$ so that a specified distribution of eigenvalues is realized; the matrices $B$ and $C$ are simply random matrices whose entries are sampled from a given probability distribution. We chose an increasing amount of states $n \in \{10, 50, 100, 500, 1000\}$ states, $m = 5$ inputs, and the intervals $[-5, -1]$ and $[-0.5, 0.5]$ bounding the real and imaginary parts of the eigenvalues of the system matrix $A$. Similarly, random initial sets and input sets are created, see [35, Sec. 3.2], represented as intervals. For the reachable set computation required for the benchmark generation, we chose an error relative to the initial set with factor $\mu = 0.1$ in [35, (12)].

### 3.3.2 Specifications

Let us denote the reachable outputs $y(t)$ as $\mathcal{Y}(t)$ and the sets of unsafe states as $\tilde{\mathcal{U}}_i$, the verification problem is to show that for a time horizon $t_f$

$$\forall t \in [0, t_f] \colon \mathcal{Y}(t) \cap \bigcup_{i=1}^{w} \tilde{\mathcal{U}}_i = \emptyset. \tag{1}$$

In case the specification should involve the reachable set of the system state instead of the system output, one can simply set $C = I$, where $I$ is the identity matrix.

RND01 Bounded time, 10 state variables, safety property (1).

RND02 Bounded time, 50 state variables, safety property (1).

RND03 Bounded time, 100 state variables, safety property (1).

RND04 Bounded time, 500 state variables, safety property (1).

RND05 Bounded time, 1000 state variables, safety property (1).

### 3.3.3 Results

The computation times of various tools for the benchmark are listed in Tab. 3.

**Note CORA** CORA applies the fully automated verification algorithm from [36].

**Note JuliaReach** We use the `GLGM06` implementation in a simple refinement loop, starting with step size $10^{-2}$, repeatedly dividing by two if the result was inconclusive, and giving up when below $10^{-5}$.

Table 3: Computation Times for the Random Benchmark in [s].

| tool | RND01 | RND02 | RND03 | RND04 | RND05 | language |
|---|---|---|---|---|---|---|
| CORA | 7.57 | 88.6 | 19.4 | 35.4 | 395.8 | MATLAB |
| JuliaReach | 13.9 | – | – | 177 | 2989 | Julia |

## 3.4 Spacecraft Rendezvous Benchmark

### 3.4.1 Model

Spacecraft rendezvous is a perfect use case for formal verification of hybrid systems since mission failure can cost lives and is extremely expensive. This benchmark is taken from [19]; its original continuous dynamics is nonlinear, and the original system is verified in the ARCH-COMP category *Continuous and Hybrid Systems with Nonlinear Dynamics*. When spacecraft are in close proximity (such as rendezvous operations), a common approximation to analyze the nonlinear dynamics is to use the linearized Clohessy-Wiltshire-Hill (CWH) equations [21]. This benchmark analyzes this linear hybrid model.

The hybrid nature of this benchmark originates from a switched controller, while the dynamics of the spacecraft is purely continuous. In particular, the modes are *approaching* (100m-1000m), *rendezvous attempt* (less than 100m), and *aborting*. For discrete-time tools, the step size 0.1 is used. The model is available in C2E2, SDVTool, and SpaceEx format on the ARCH website[2]. The set of initial states is

$$\mathcal{X}_0 = \begin{bmatrix} -900 \\ -400 \\ 0 \\ 0 \end{bmatrix} \oplus \begin{bmatrix} [-25, 25] \\ [-25, 25] \\ 0 \\ 0 \end{bmatrix}.$$

The following benchmark instances are considered:

SRNA01 The spacecraft approaches the target as planned and there exists no transition into the *aborting* mode.

SRA01 A transition into *aborting* mode occurs at time $t = 120$ [min].

SRA02 A transition into *aborting* mode occurs nondeterministically, $t \in [120, 125]$ [min].

SRA03 A transition into *aborting* mode occurs nondeterministically, $t \in [120, 145]$ [min].

SRA04 A transition into *aborting* mode occurs at time $t = 240$ [min].

SRA05 A transition into *aborting* mode occurs nondeterministically, $t \in [235, 240]$ [min].

[2] cps-vo.org/node/36349

SRA06 A transition into *aborting* mode occurs nondeterministically, $t \in [230, 240]$ [min].

SRA07 A transition into *aborting* mode occurs nondeterministically, $t \in [50, 150]$ [min].

SRA08 A transition into *aborting* mode occurs nondeterministically, $t \in [0, 240]$ [min].

An initial, discrete-time analysis indicated it is safe to enter the *aborting* mode up to around time $t = 250$ [min]. We also added the following two instances, which are presumably unsafe. For timing, tools should use the same settings for these as for the safe cases.

SRU01 A transition into *aborting* mode occurs at time $t = 260$ [min].

SRU02 A transition into *aborting* mode occurs nondeterministically, $t \in [0, 260]$ [min].

### 3.4.2 Specifications

Given the thrust constraints of the specified model, in mode *rendezvous attempt*, the absolute velocity must stay below 0.055 m/s. In the *aborting* mode, the vehicle must avoid the target, which is modeled as a box $\mathcal{B}$ with 0.2 m edge length and the center placed as the origin. In the *rendezvous attempt* the spacecraft must remain within the line-of-sight cone $\mathcal{L} = \{[x, y]^T \mid (x \geq -100\,m) \wedge (y \geq x \tan(30°)) \wedge (-y \geq x \tan(30°))\}$. It is sufficient to check these parameters for a time horizon of 300 minutes.

Let us denote the discrete state by $z(t)$ and the continuous state vector by $x(t) = [s_x, s_y, v_x, v_y]^T$, where $s_x$ and $s_y$ are the positions in x- and y-direction, respectively, and $v_x$ and $v_y$ are the velocities in x- and y-direction, respectively. The mode *approaching* is denoted by $z_1$, the mode *rendezvous attempt* by $z_2$, and the mode *aborting* by $z_3$. We can formalize the specification as

SR02 $\forall t \in [0, 300\,min], \forall x(0) \in \mathcal{X}_0 : (z(t) = z_2) \implies \Big(\sqrt{v_x^2 + v_y^2} \leq 0.055\,m/s \wedge [s_x, s_y]^T \in \mathcal{L}\Big) \wedge (z(t) = z_3) \implies ([s_x, s_y]^T \notin \mathcal{B})$.

To solve the above specification, all tools under-approximate the nonlinear constraint $\sqrt{v_x^2 + v_y^2} \leq 0.055\,m/s$ by an octagon as shown in Fig. 3.

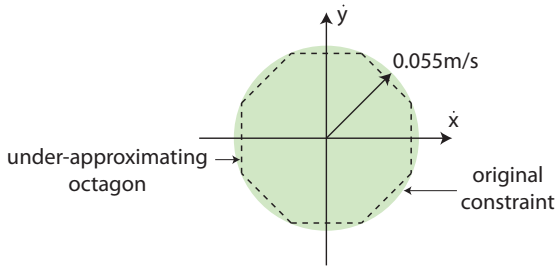


Figure 3: Under-approximation of the nonlinear velocity constraint by an octagon.

**Remark on nonlinear constraint** In the original benchmark, the constraint on the velocity was set to 0.05 m/s, but it can be shown that this constraint cannot be satisfied by a counterexample. For this reason, we have relaxed the constraint to 0.055 m/s.

### 3.4.3 Results

Results of the spacecraft rendezvous benchmark for the $s_x$-$s_y$-plane are shown for the version SRNA01 in Fig. 4 and for the version SRA01 in Fig. 5. The computation times of various tools for the spacecraft rendezvous benchmark are listed in Tab. 4.

**Note CORA** For both benchmark versions, CORA was run with a zonotope order of 10 and with the following step sizes: 0.2 [min] for the mode *approaching*, 0.02 [min] for the mode *rendezvous attempt*, and 0.2 [min] for the mode *aborting* (does not exist for version SRNA01). Intersections with deterministic guards are calculated with the method of Girard and Le Guernic in [26]. In order to find suitable orthogonal directions for the method in [26], we perform the following procedure: first, we project the last zonotope not intersecting the guard set onto the guard set; second, we apply principal component analysis to the generators of the projected zonotope, providing us with the orthogonal directions. For non-deterministic guards we first unite all reachable sets intersecting the guard set and then compute the intersection using constrained zonotopes [33].

**Note JuliaReach** We use the `BFFPSV18` algorithm with a one-block partition and hyperrectangular reach sets with step size 0.04 for most instances. We handle discrete transitions by computing the intersection with invariants and guards lazily before their overapproximation with hyperrectangles. For the instance SRA04, we use a clustering strategy of order 40 and step size 0.01.

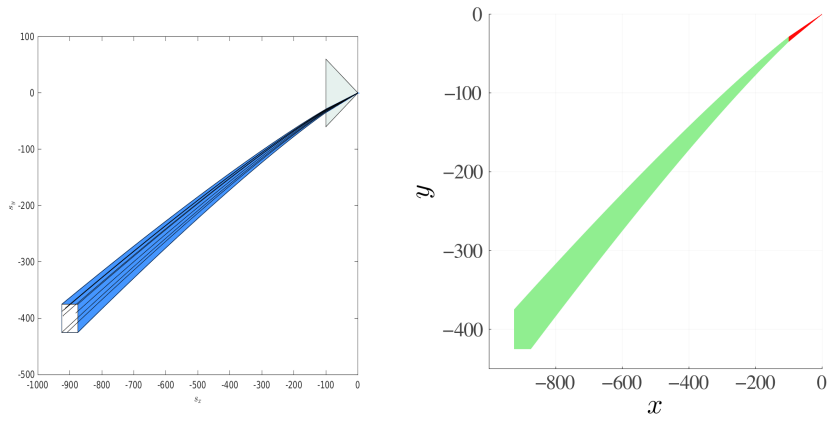


(a) CORA. (b) JuliaReach.

Figure 4: Reachable sets for the spacecraft rendezvous benchmark in the $s_x$-$s_y$-plane for the benchmark variant without maneuver abortion (SRNA01).

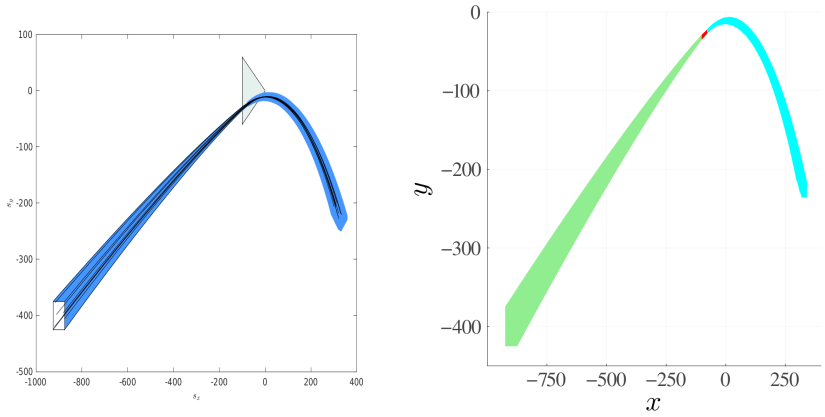


(a) CORA. (b) JuliaReach.

Figure 5: Reachable sets for the spacecraft rendezvous benchmark in the $s_x$-$s_y$-plane for the benchmark variant with maneuver abortion at $t = 120$ [min] (SRA01, over analysis time horizon of 300 [min])

Table 4: Computation time [s] for the spacecraft rendezvous benchmarks (**SR***) for specification **SR02**.

| **tool** | **NA01** | **A01** | **A02** | **A03** | **A04** | **A05** | **A06** | **A07** | **A08** | **U01** | **U02** |
|---|---|---|---|---|---|---|---|---|---|---|---|
| CORA | 19.24 | 5.02 | 7.72 | 12.20 | 15.55 | 29.07 | 29.43 | 91.47 | 203.9 | 17.54 | 207.82 |
| JuliaReach | 0.88 | 1.02 | 1.08 | 1.51 | 93.5 | – | – | – | – | 11.4 | 16.7 |
| | *discrete-time tools* | | | | | | | | | | |
| JuliaReach | 0.35 | 0.37 | 0.45 | 0.59 | – | – | – | – | – | – | 9.6 |

## 3.5 Powertrain with Backlash

### 3.5.1 Model

The powertrain benchmark is an extensible benchmark for hybrid systems with linear continuous dynamics taken from [7, Sec. 6] and [13, Sec. 4]. The essence of this benchmark is recalled here, and the reader is referred to the above-cited papers for more details. The benchmark considers the powertrain of a vehicle consisting of its motor and several rotating masses representing different components of the powertrain, e.g., gears, differential, and clutch, as illustrated in Fig. 6. The benchmark is extensible in the sense that the number of continuous states can be easily extended to $n = 7+2\theta$, where $\theta$ is the number of additional rotating masses. The number of discrete modes, however, is fixed and originates from backlash, which is caused by a physical gap between two components that are normally touching, such as gears. When the rotating components switch direction, for a short time they temporarily disconnect, and the system is said to be in the *dead zone*. The model is available in SpaceEx format on the ARCH website[3].

[3] cps-vo.org/node/49115

The set of initial states is

$$\begin{aligned}\mathcal{X}_0 &= \{c + \alpha g \mid \alpha \in [-1, 1]\},\\ c &= [-0.0432, -11, 0, 30, 0, 30, 360, -0.0013, 30, \ldots, -0.0013, 30]^T,\\ g &= [0.0056, 4.67, 0, 10, 0, 10, 120, 0.0006, 10, \ldots, 0.0006, 10]^T.\end{aligned}$$

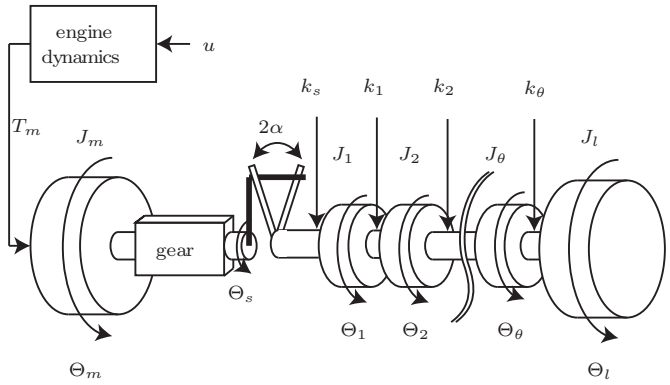


Figure 6: Powertrain model.

### 3.5.2 Specifications

We analyze an extreme maneuver from a maximum negative acceleration that lasts for 0.2 [s], followed by a maximum positive acceleration that lasts for 1.8 [s]. The initial states of the model are on a line segment in the $n$-dimensional space. We create different difficulty levels of the reachability problem by scaling down the initial states by some percentage. The model has the following non-formal specification: after the change of direction of acceleration, the powertrain completely passes the dead zone before being able to transmit torque again. Due to oscillations in the torque transmission, the powertrain should not re-enter the dead zone of the backlash.

To formalize the specification using signal temporal logic (STL), let us introduce the following discrete states:

- $z_1$ : left contact zone
- $z_2$ : dead zone
- $z_3$ : right contact zone

For all instances, the common specification is: $G_{[0,0.2]}(z_1 U \big(z_2 U z_3\big)) U (G z_3)$, where $U$ and $G$ denote the *until* and *globally* operators, respectively, and subscripted intervals restrict the time interval of the temporal operators, see, e.g., [31, Sec. 2.2]. The instances only differ in the size of the system and the initial set, where $\texttt{center}(\cdot)$ returns the volumetric center of a set.

DTN01 $\theta = 2$, $\mathcal{X}_0 := 0.05(\mathcal{X}_0 - \texttt{center}(\mathcal{X}_0)) + \texttt{center}(\mathcal{X}_0)$.

DTN02 $\theta = 2$, $\mathcal{X}_0 := 0.3(\mathcal{X}_0 - \texttt{center}(\mathcal{X}_0)) + \texttt{center}(\mathcal{X}_0)$.

DTN03 $\theta = 2$, no change of $\mathcal{X}_0$.

DTN04 $\theta = 22$, $\mathcal{X}_0 := 0.05(\mathcal{X}_0 - \texttt{center}(\mathcal{X}_0)) + \texttt{center}(\mathcal{X}_0)$.

DTN05 $\theta = 22$, $\mathcal{X}_0 := 0.3(\mathcal{X}_0 - \texttt{center}(\mathcal{X}_0)) + \texttt{center}(\mathcal{X}_0)$.

DTN06 $\theta = 22$, no change of $\mathcal{X}_0$.

### 3.5.3 Results

Results of the powertrain benchmark in the $x_1$-$x_3$-plane are shown in Fig. 7. The computation times of various tools for the powertrain benchmark are listed in Tab. 5.

**Note CORA** CORA uses the following time step sizes: 0.0005s for DTN01, DTN02, and DTN03; 0.0002s for DTN04 and DTN05; and 0.0001s for DTN06. For all benchmark versions, CORA was run with a zonotope order of 20. The intersections with the guard sets are calculated with the approach from [26], and principal component analysis is used to find suitable directions for the enclosure of the guard intersections.

**Note JuliaReach** We use the `GLGM06` algorithm. In addition, we use slightly different analysis parameters for different modes, e.g., step sizes varying between 0.002 and 0.03.

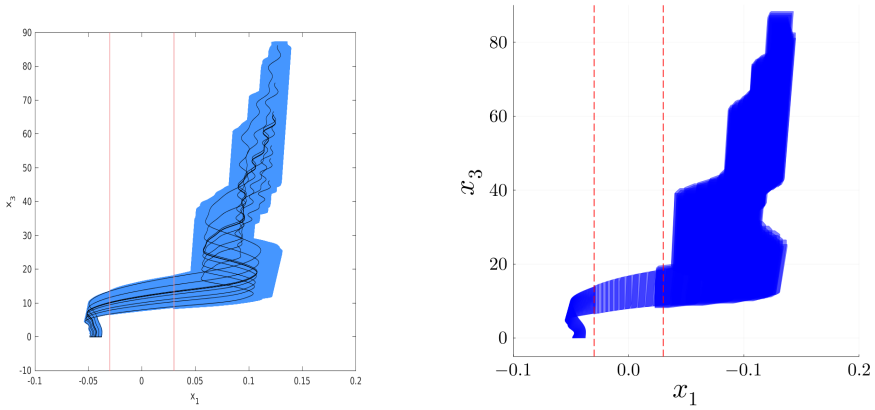


(a) CORA (DTN03). (b) JuliaReach (DTN03).

Figure 7: Reachable sets in the $x_1$-$x_3$-plane.

Table 5: Computation Times for the Powertrain Benchmark in [s].

| **tool** | **DTN01** | **DTN02** | **DTN03** | **DTN04** | **DTN05** | **DTN06** | **language** |
|---|---|---|---|---|---|---|---|
| CORA | 7.52 | 6.83 | 7.05 | 43.2 | 91.1 | 242.9 | MATLAB |
| JuliaReach | 0.004 | 0.005 | 0.045 | 0.006 | 0.023 | 0.01 | Julia |

## 3.6 Platooning Benchmark

### 3.6.1 Model

The platooning benchmark considers a platoon of three vehicles following each other. This benchmark considers loss of communication between vehicles. The initial discrete state is $q_c$. Three scenarios are considered for the loss of communication:

PLAA01 (arbitrary loss) The loss of communication can occur at any time, see Fig. 8(a). This includes the possibility of no communication at all.

PLADxy (loss at deterministic times) The loss of communication occurs at fixed points in time, which are determined by clock constraints $c_1$ and $c_2$ in Fig. 8(b). The clock $t$ is reset when communication is lost and when it is re-established. Note that the transitions have must-semantics, i.e., they take place as soon as possible.

PLAD01: $c_1 = c_2 = 5$.

PLANxy (loss at nondeterministic times) The loss of communication occurs at any time $t \in [t_b, t_c]$ in Fig. 8(c). The clock $t$ is reset when communication is lost and when it is re-established. Communication is reestablished at any time $t \in [0, t_r]$. This scenario covers loss of communication after an arbitrarily long time $t \geq t_c$ by reestablishing communication in zero time.

PLAN01: $t_b = 10$, $t_c = 20$, $t_r = 20$.

The models are available in SpaceEx, KeYmaera, and MATLAB/Simulink format on the ARCH website[4]. For discrete-time tools, the step size 0.1 is used.

**Discussion** The arbitrary-loss scenario (PLAA) subsumes the other two instances (PLAD, PLAN).

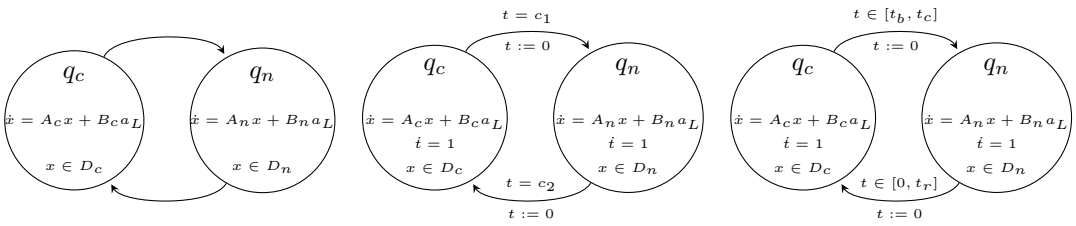


(a) Arbitrary switching. (b) Deterministic switching. (c) Nondeterministic switching.

Figure 8: Three options adapted from the original benchmark proposal [15]. On the left, the system can switch arbitrarily between the modes. In the middle, mode switches are only possible at given points in time. On the right, mode switches are only possible during given time intervals.

[4] cps-vo.org/node/15096

### 3.6.2 Specifications

The verification goal is to check whether the minimum distance between vehicles is preserved. The choice of the coordinate system is such that the minimum distance is a negative value.

BNDxy Bounded time (no explicit bound on the number of transitions): For all $t \in [0, 20]$ [s], $x_1(t) \geq -d_{min}$ [m], $x_4(t) \geq -d_{min}$ [m], and $x_7(t) \geq -d_{min}$ [m].

BND50: $d_{min} = 50$.

BND42: $d_{min} = 42$.

BND30: $d_{min} = 30$.

UNBxy Unbounded time and unbounded switching: For all $t \geq 0$ [s], $x_1(t) \geq -d_{min}$ [m], $x_4(t) \geq -d_{min}$ [m], and $x_7(t) \geq -d_{min}$ [m].

UNB50: $d_{min} = 50$.

UNB42: $d_{min} = 42$.

UNB30: $d_{min} = 30$.

### 3.6.3 Results

Results of the platoon benchmark for state $x_1$ over time are shown in Fig. 9-11. The computation times of various tools for the platoon benchmark are listed in Tab. 6.

**Note CORA** CORA was run with the following settings:

- PLAA01-BND50: zonotope order 400 and time step size 0.02s.
- PLAA01-BND42: zonotope order 800 and time step size 0.009s.
- PLAD01-BND42: zonotope order 20 and time step size 0.02s.
- PLAD01-BND30: zonotope order 200 and time step size 0.02s.
- PLAN01-UNB50: zonotope order 400 and time step size 0.01s. To verify the specification for all times, the reachable set was increased by 1% at $t = 50$ and it was checked whether this set is re-entered.
- PLAA01: we used *continuization* [8, 9] to rewrite the hybrid automaton as a purely continuous system with uncertain parameters.

**Note JuliaReach** For PLAD01-BND42, we use the `BFFPSV18` algorithm with a one-block partition, hyperrectangular reach sets, and step size 0.01. For PLAD01-BND30, we use the `LGG09` algorithm with step size 0.03, and intersections with the guard are taken lazily with an octagonal template.

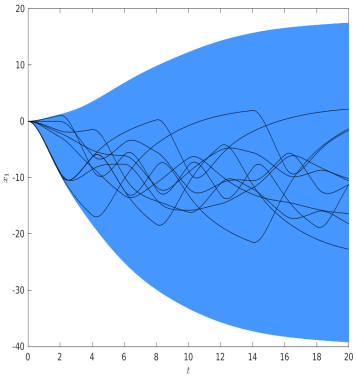

(a) CORA.

Figure 9: PLAA01: Reachable sets of $x_1$ plotted over time. CORA additionally shows possible trajectories.

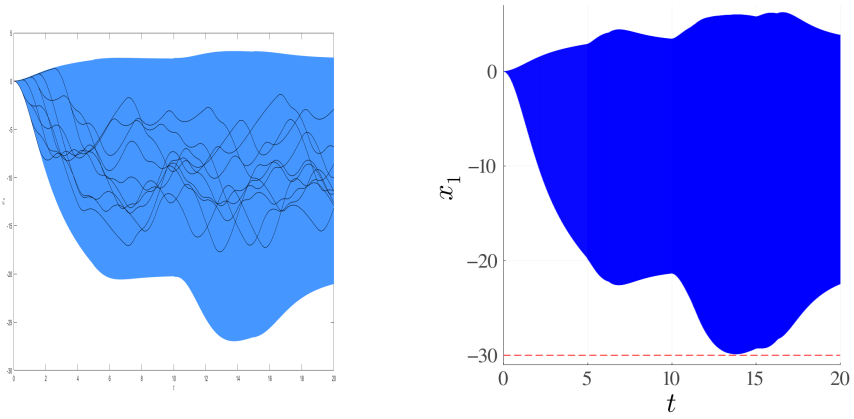


(a) CORA (BND30). (b) JuliaReach (BND30).

Figure 10: PLAD01: Reachable sets of $x_1$ plotted over time. CORA additionally shows possible trajectories.

## 3.7 Gearbox Benchmark

### 3.7.1 Model

The gearbox benchmark models the motion of two meshing gears. When the gears collide, an elastic impact takes place. As soon as the gears are close enough, the gear is considered *meshed*. The model includes a monitor state that checks whether the gears are meshed or free and is available in SpaceEx format[5] and as a Simulink model[6]. Once the monitor reaches the state *meshed*, it stays there indefinitely.

[5] cps-vo.org/node/34375
[6] cps-vo.org/node/34374

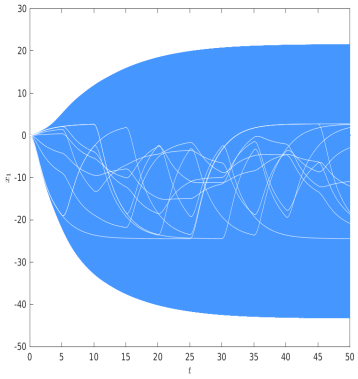


Figure 11: PLAN01: Reachable sets of $x_1$ plotted over time using CORA.

Table 6: Computation Times for the Platoon Benchmark in [s].

| **tool** | **PLAA01 BND50** | **PLAA01 BND42** | **PLAD01 BND42** | **PLAD01 BND30** | **PLAN01 UNB50** | **language** |
|---|---|---|---|---|---|---|
| CORA | 11.6 | 43.1 | 1.16 | 2.29 | 154 | MATLAB |
| JuliaReach | – | – | 0.05 | 66.8 | – | Julia |
| | *discrete-time tools* | | | | | |
| JuliaReach | – | – | 0.84 | 1.04 | – | Julia |

With four continuous state variables, the gearbox benchmark has a relatively low number of continuous state variables. The challenging aspect of this benchmark is that the solution heavily depends on the initial state as already pointed out in [20]. For some initial continuous states, the target region is reached without any discrete transition, while for other initial states, several discrete transitions are required.

In the original benchmark, the position uncertainty in the direction of the velocity vector of the gear teeth (x-direction) is across the full width of the gear spline. Uncertainties of the position and velocity in y-direction, which is perpendicular to the x-direction, are considered to be smaller. Due to the sensitivity with respect to the initial set, we consider smaller initial sets. The full uncertainty in x-direction could be considered by splitting the uncertainty in x-direction and aggregating the individual results. For discrete-time tools, the step size $10^{-4}$ is used.

GRBX01: The initial set is $\mathcal{X}_0 = 0 \times 0 \times [-0.0168, -0.0166] \times [0.0029, 0.0031] \times 0$.

GRBX02: The initial set is $\mathcal{X}_0 = 0 \times 0 \times [-0.01675, -0.01665] \times [0.00285, 0.00315] \times 0$.

### 3.7.2 Specification

The goal is to show that the gears are *meshed* within a time frame of 0.2 [s] and that the bound $x_5 \leq 20$ [Nm] of the cumulated impulse is met. Using the monitor states *free* and *meshed*, and a global clock $t$, this can be expressed as a safety property as follows: For all $t \geq 0.2$, the monitor should be in *meshed*. Under nonblocking assumptions, this means that $t < 0.2$ whenever the monitor is not in *meshed*, i.e., when it is in *free*.

MES01: forbidden states: $(\mathit{free} \wedge t \geq 0.2) \vee (x_5 \geq 20)$

### 3.7.3 Results

Results of the benchmark for state $x_3$ and $x_4$ are shown in Fig. 12. The computation times of various tools for the benchmark are listed in Tab. 7.

**Note CORA** CORA was run with a time step size of 0.0011 and a zonotope order of 20. The intersections with the guard sets were calculated with the method of Girard and Le Guernic [26]. In order to find suitable orthogonal directions for the method in [26], we perform the following procedure: first, we project the last zonotope not intersecting the guard set onto the guard set; second, we apply principal component analysis to the generators of the projected zonotope, providing us with the orthogonal directions.

**Note JuliaReach** We use the `LGG09` algorithm with step size 0.0008.

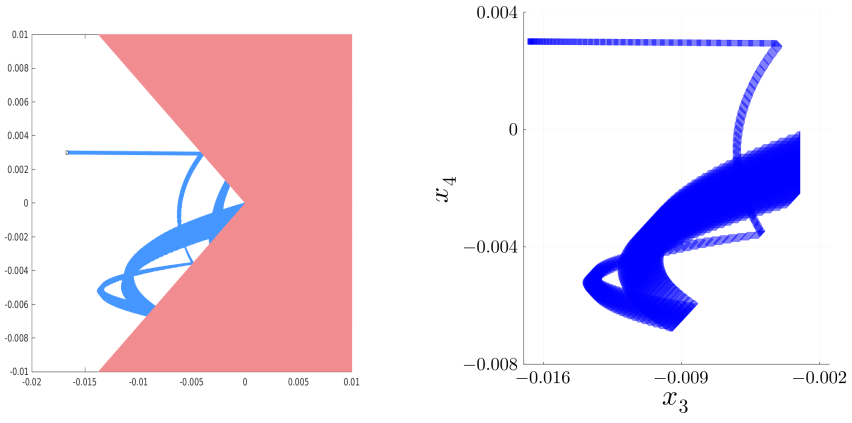


(a) CORA. (b) JuliaReach.

Figure 12: Gearbox (GRBX01): Reachable sets of $x_3$ and $x_4$.

Table 7: Computation Times of the Gearbox Benchmark in [s].

| tool | GRBX01-MES01 | GRBX02-MES01 | language |
|---|---|---|---|
| CORA | 1.87 | 1.49 | MATLAB |
| JuliaReach | 2.83 | 2.86 | Julia |
| | *discrete-time tools* | | |
| JuliaReach | 16.1 | 15.9 | Julia |

## 3.8 Brake Benchmark

### 3.8.1 Model

The brake benchmark models an electro-mechanical braking system, where a motor pushes a brake caliper against a brake disk that is connected to a (car) wheel [34]. The model describes a closed-loop system comprising a plant model as well as a controller and is representative for challenges in automotive systems. The original Simulink model has been simplified for usage in various analysis tools[7]. Here, we consider a linearized version with parameters.

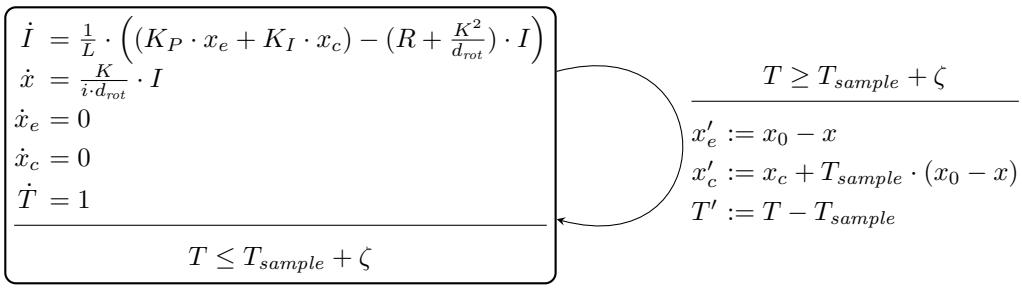


Figure 13: Hybrid automaton of the electro-mechanical brake with periodic discrete-time PI controller and sampling jitter.

The model is a hybrid automaton (see Fig. 13) with four state variables (the motor current $I$, the brake position $x$, and two auxiliary linearization variables) and a clock variable $T$. The automaton consists of a single mode and a self-loop transition. The transition is time-triggered, i.e., it only depends on the value of the clock variable.

We consider two types of uncertainties in the model. The first uncertainty is a variation in the model parameters. We use the settings from [34] for the nonparametric and parametric scenarios. The second uncertainty is sampling jitter (i.e., nondeterministic switching). Unlike the linear model in [34], we consider jitter with a periodic clock (instead of a drifting clock). For discrete-time tools, the step size $10^{-8}$ is used.

[7] cps-vo.org/node/20289

### 3.8.2 Specification

While structurally simple, the benchmark is challenging due to the large number of 1,001 discrete jumps within the time horizon 0.1. The initial state is the origin, we use the parameters $x_0 = 0.05$ and $T_{sample} = 10^{-4}$, and in the case of nondeterministic switching the transitions are taken at multiples of $T_{sample}$ with a nondeterministic jitter from the interval $\zeta = [-10^{-8}, 10^{-7}]$. We study the property $x < x_0$ in both scenarios without and with parameter ranges:

BRKDC01: Verify that $x < x_0$ holds for the whole time horizon 0.1 (non-parametric scenario with deterministic switching).

BRKNC01: Same as BRKDC01, but with non-deterministic switching.

BRKNP01: Report the largest time horizon for which $x < x_0$ holds (parametric scenario with non-deterministic switching).

### 3.8.3 Results

Results of the benchmark are shown in Fig. 14. The computation times of various tools for the benchmark are listed in Tab. 8.

**Note CORA** CORA was run with a time step size of $2^{-5}$, a zonotope order of 20, and the intersections with the non-deterministic guard sets were calculated with constrained zonotopes [33].

**Note JuliaReach** For the BRKDC01 and BRKNC01 scenario, we use the `GLGM06` algorithm with fixed step sizes $2 \cdot 10^{-7}$ resp. $7 \cdot 10^{-8}$. For the BRKNP01 scenario, we use the `ASB07` algorithm with step size $10^{-8}$. In all scenarios, we use the maximum zonotope order 1 (i.e., boxes). We use a custom analysis for dealing with the time-triggered transition efficiently, considering intersections with the guard separately from the flowpipe computation, as described in [22]. The largest time horizon for which we can prove $x < x_0$ in the BRKNP01 scenario is 0.0824 s, both in dense and discrete time.

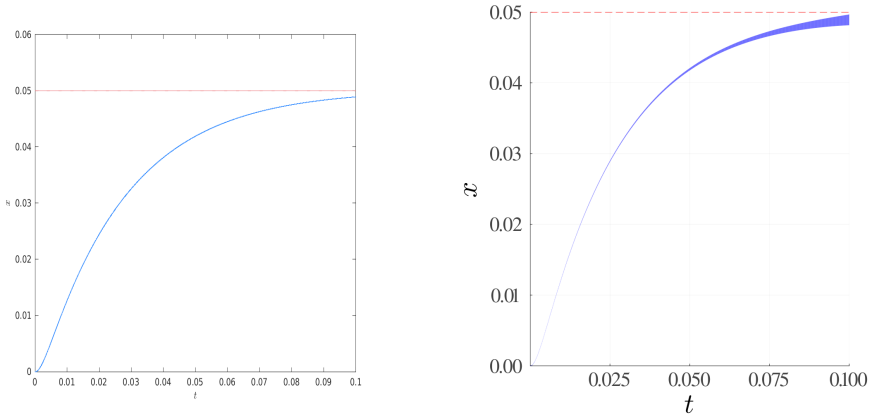


(a) CORA. (b) JuliaReach.

Figure 14: Brake: Reachable sets for $x$ over time.

Table 8: Computation Times of the Brake Benchmark in [s].

| tool | BRKDC01 | BRKNC01 | BRKP01 | language |
|---|---|---|---|---|
| CORA | 11.13 | 9.82 | 52.2 | MATLAB |
| JuliaReach | 0.11 | 1.14 | 11.9 | Julia |
| | *discrete-time tools* | | | |
| JuliaReach | 0.97 | 0.97 | 8.09 | Julia |

# 4 Conclusion and Outlook

This report presents the results of the ninth friendly competition for the formal verification of continuous and hybrid systems with linear continuous dynamics as part of the ARCH'25 workshop. The reports of other categories can be found in the proceedings and on the ARCH website: cps-vo.org/group/ARCH.

A main observation of the 2025 edition is that much harder randomly generated benchmarks could be solved. One can execute the dockerfiles of all tools on gitlab.com/goranf/ARCH-COMP. Information about the competition in 2026 will be announced on the ARCH website.

# 5 Acknowledgments

Matthias Althoff and Maximilian Perschl gratefully acknowledge financial support by the project ConVeY funded by the German Research Foundation (DFG) under grant number GRK 2428.

Christian Schilling acknowledges support from the Independent Research Fund Denmark under reference number 10.46540/3120-00041B and the Villum Investigator Grant S4OS under reference number 37819.

# References

[1] M. Althoff. *Reachability Analysis and its Application to the Safety Assessment of Autonomous Cars.* Dissertation, Technische Universität München, 2010. http://nbn-resolving.de/urn/resolver.pl?urn:nbn:de:bvb:91-diss-20100715-963752-1-4.

[2] M. Althoff. An introduction to CORA 2015. In *Proc. of the Workshop on Applied Verification for Continuous and Hybrid Systems*, pages 120–151, 2015.

[3] M. Althoff. Reachability analysis of large linear systems with uncertain inputs in the Krylov subspace. *IEEE Transactions on Automatic Control*, 65(2):477–492, 2020.

[4] M. Althoff. Guaranteed state estimation in CORA 2021. In *Proc. of the 8th International Workshop on Applied Verification of Continuous and Hybrid Systems*, pages 161–175, 2021.

[5] M. Althoff and D. Grebenyuk. Implementation of interval arithmetic in CORA 2016. In *Proc. of the 3rd International Workshop on Applied Verification for Continuous and Hybrid Systems*, pages 91–105, 2016.

[6] M. Althoff, D. Grebenyuk, and N. Kochdumper. Implementation of Taylor models in CORA 2018. In *Proc. of the 5th International Workshop on Applied Verification for Continuous and Hybrid Systems*, pages 145–173, 2018.

[7] M. Althoff and B. H. Krogh. Avoiding geometric intersection operations in reachability analysis of hybrid systems. In *Hybrid Systems: Computation and Control*, pages 45–54, 2012.

[8] M. Althoff, C. Le Guernic, and B. H. Krogh. Reachable set computation for uncertain time-varying linear systems. In *Hybrid Systems: Computation and Control*, pages 93–102, 2011.

[9] M. Althoff, A. Rajhans, B. H. Krogh, S. Yaldiz, X. Li, and L. Pileggi. Formal verification of phase-locked loops using reachability analysis and continuization. *Communications of the ACM*, 56(10):97–104, 2013.

[10] M. Althoff, O. Stursberg, and M. Buss. Reachability analysis of linear systems with uncertain parameters and inputs. In *Proc. of the 46th IEEE Conference on Decision and Control*, pages 726–732, 2007.

[11] Matthias Althoff. Checking and establishing reachset conformance in CORA 2023. In *Proc. of 10th International Workshop on Applied Verification of Continuous and Hybrid Systems*, volume 96 of *EPiC Series in Computing*, pages 9–33, 2023.

[12] Matthias Althoff, Marcelo Forets, Christian Schilling, and Mark Wetzlinger. ARCH-COMP24 category report: Continuous and hybrid systems with linear continuous dynamics. In Goran Frehse and Matthias Althoff, editors, *Proc. of the 11th Int. Workshop on Applied Verification for Continuous and Hybrid Systems*, volume 103 of *EPiC Series in Computing*, pages 15–38. EasyChair, 2024.

[13] S. Bak, S. Bogomolov, and M. Althoff. Time-triggered conversion of guards for reachability analysis of hybrid automata. In *Proc. of the 15th International Conference on Formal Modelling and Analysis of Timed Systems*, pages 133–150, 2017.

[14] Stanley Bak, Hoang-Dung Tran, and Taylor T. Johnson. Numerical verification of affine systems with up to a billion dimensions. In *Proc. of the 22nd ACM International Conference on Hybrid Systems: Computation and Control*, pages 23–32, 2019.

[15] I. Ben Makhlouf and S. Kowalewski. Networked cooperative platoon of vehicles for testing methods and verification tools. In *Proc. of ARCH14-15. 1st and 2nd International Workshop on Applied veRification for Continuous and Hybrid Systems*, pages 37–42, 2015.

[16] Sergiy Bogomolov, Marcelo Forets, Goran Frehse, Andreas Podelski, and Christian Schilling. Decomposing reach set computations with low-dimensional sets and high-dimensional matrices. *Inf. Comput.*, 2022.

[17] Sergiy Bogomolov, Marcelo Forets, Goran Frehse, Kostiantyn Potomkin, and Christian Schilling. JuliaReach: a toolbox for set-based reachability. In *HSCC*, pages 39–44. ACM, 2019.

[18] Sergiy Bogomolov, Marcelo Forets, Goran Frehse, Frédéric Viry, Andreas Podelski, and Christian Schilling. Reach set approximation through decomposition with low-dimensional sets and high-dimensional matrices. In *HSCC*, pages 41–50. ACM, 2018.

[19] N. Chan and S. Mitra. Verifying safety of an autonomous spacecraft rendezvous mission. In *Proc. of the 4th International Workshop on Applied Verification of Continuous and Hybrid Systems*, pages 20–32, 2017.

[20] H. Chen, S. Mitra, and G. Tian. Motor-transmission drive system: a benchmark example for safety verification. In *Proc. of ARCH14-15. 1st and 2nd International Workshop on Applied veRification for Continuous and Hybrid Systems*, pages 9–18, 2015.

[21] W. H. Clohessy and R. S. Wiltshire. Terminal guidance system for satellite rendezvous. 27(9):653–658.

[22] Marcelo Forets, Daniel Freire, and Christian Schilling. Efficient reachability analysis of parametric linear hybrid systems with time-triggered transitions. In *MEMOCODE*, pages 1–6. IEEE, 2020.

[23] Marcelo Forets and Christian Schilling. LazySets.jl: Scalable symbolic-numeric set computations. *Proceedings of the JuliaCon Conferences*, 1(1):11, 2021.

[24] Marcelo Forets and Christian Schilling. Conservative time discretization: A comparative study. In *iFM*, volume 13274 of *LNCS*, pages 149–167. Springer, 2022.

[25] Victor Gaßmann and Matthias Althoff. Implementation of ellipsoidal operations in CORA 2022. In *Proc. of 9th International Workshop on Applied Verification of Continuous and Hybrid Systems*, pages 1–17, 2022.

[26] A. Girard and C. Le Guernic. Zonotope/hyperplane intersection for hybrid systems reachability analysis. In *Proc. of Hybrid Systems: Computation and Control*, LNCS 4981, pages 215–228. Springer, 2008.

[27] Antoine Girard, Colas Le Guernic, and Oded Maler. Efficient computation of reachable sets of linear time-invariant systems with inputs. In *HSCC*, volume 3927 of *LNCS*, pages 257–271. Springer, 2006.

[28] Z. Han and B. H. Krogh. Reachability analysis of large-scale affine systems using low-dimensional polytopes. In *Hybrid Systems: Computation and Control*, LNCS 3927, pages 287–301. Springer, 2006.

[29] Colas Le Guernic and Antoine Girard. Reachability analysis of linear systems using support functions. *Nonlinear Analysis: Hybrid Systems*, 4(2):250–262, 2010. IFAC World Congress 2008.

[30] Mohammad Mahdi Malakiyeh, Saeed Shojaee, and Klaus-Jürgen Bathe. The bathe time integration method revisited for prescribing desired numerical dissipation. *Computers & Structures*, 212:289–298, 2019.

[31] Oded Maler and Dejan Nickovic. Monitoring temporal properties of continuous signals. In *Proc. of Formal Techniques, Modelling and Analysis of Timed and Fault-Tolerant Systems*, pages 152–166, 2004.

[32] Christopher Rackauckas and Qing Nie. DifferentialEquations.jl – a performant and feature-rich ecosystem for solving differential equations in Julia. *The Journal of Open Research Software*, 5(1), 2017.

[33] J. K. Scott, D. M. Raimondo, G. R. Marseglia, and R. D. Braatz. Constrained zonotopes: A new tool for set-based estimation and fault detection. *Automatica*, 69:126–136, 2016.

[34] Thomas Strathmann and Jens Oehlerking. Verifying properties of an electro-mechanical braking system. In *ARCH@CPSWeek*, volume 34 of *EPiC Series in Computing*, pages 49–56. EasyChair, 2015.

[35] Mark Wetzlinger and Matthias Althoff. Randomized generation of arbitrarily difficult verification benchmarks for linear time-invariant systems. In Goran Frehse and Matthias Althoff, editors, *Proc. of the 11th Int. Workshop on Applied Verification for Continuous and Hybrid Systems*, volume 103 of *EPiC Series in Computing*, pages 153–162. EasyChair, 2024.

[36] Mark Wetzlinger, Niklas Kochdumper, Stanley Bak, and Matthias Althoff. Fully-automated verification of linear systems using reachability analysis with support functions. In *Proc. of the 26th ACM International Conference on Hybrid Systems: Computation and Control*, 2023.

[37] Mark Wetzlinger, Viktor Kotsev, Adrian Kulmburg, and Matthias Althoff. Implementation of polyhedral operations in CORA 2024. In Goran Frehse and Matthias Althoff, editors, *Proc. of the 11th Int. Workshop on Applied Verification for Continuous and Hybrid Systems*, volume 103 of *EPiC Series in Computing*, pages 163–181. EasyChair, 2024.